The American Journal of Human Genetics, Volume *99*

Supplemental Data

GNA14 Somatic Mutation Causes Congenital and Sporadic Vascular Tumors by MAPK Activation

Young H. Lim, Antonella Bacchiocchi, Jingyao Qiu, Robert Straub, Anna Bruckner, Lionel Bercovitch, Deepak Narayan, Yale Center for Mendelian Genomics, Jennifer McNiff, Christine Ko, Leslie Robinson-Bostom, Richard Antaya, Ruth Halaban, and Keith A. Choate

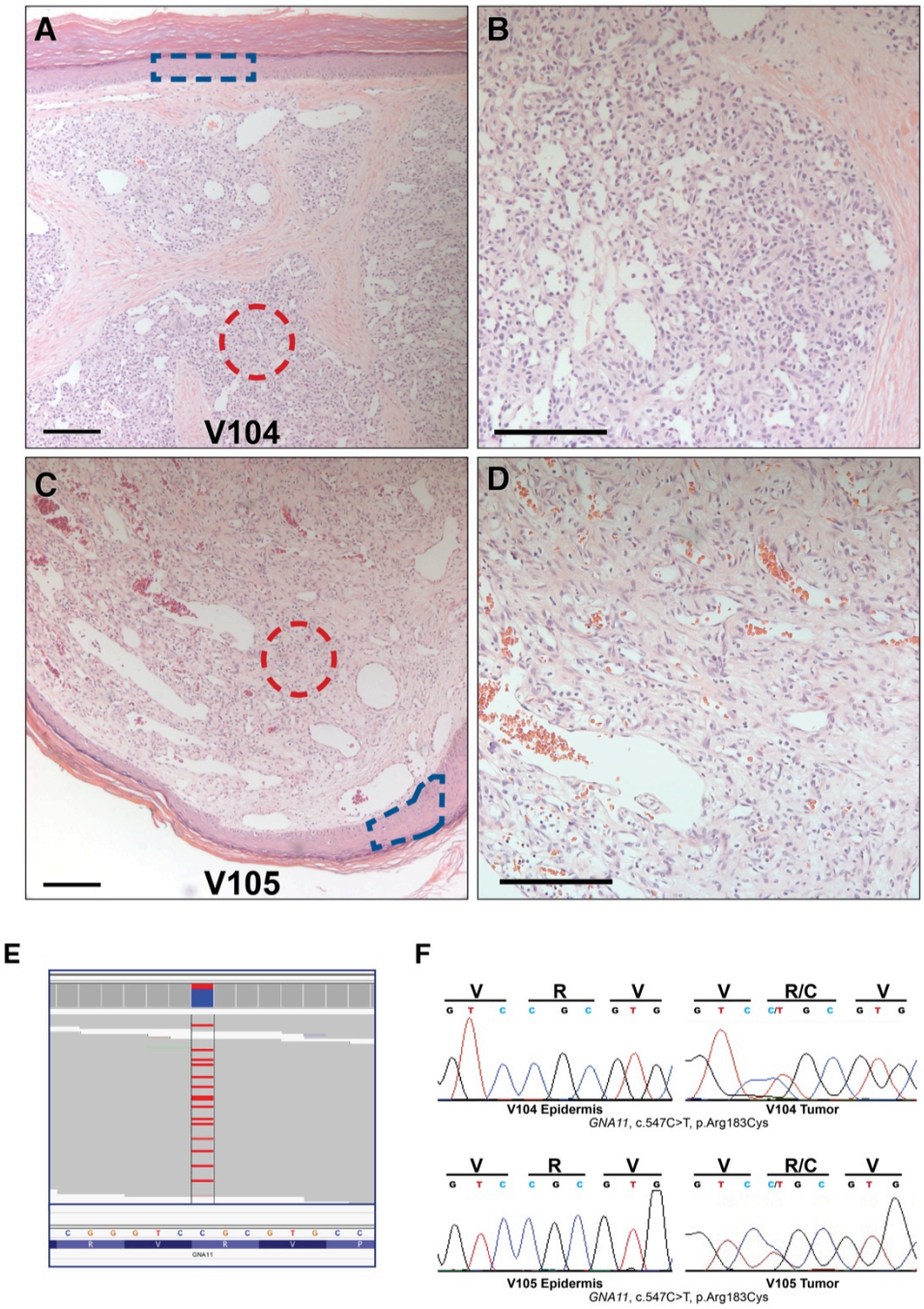

Figure S1. Somatic *GNA11* c.547C>T (p.Arg183Cys) mutation causes sporadic lobular capillary hemangiomas. (A-D) V104 and V105 are sporadic lobular capillary hemangiomas with histology at **(A,C)** 10X and **(B,D)** 20X magnification showing classic keratinized encapsulation of proliferating lobular capillaries. Areas where LCM was employed to isolate tissue for DNA is shown for unaffected epidermis (blue boxes), and tumor (red circles). **(E)** IGV of V104 exome data demonstrates 16/71 (22%) non-reference reads corresponding to c.547C>T (p.Arg183Cys). **(F)** Sanger sequencing of unaffected epidermis and tumor of V104 and V105 shows *GNA11* c.547C>T (p.Arg183Cys) in tumor only. Scale bars = 150μm.

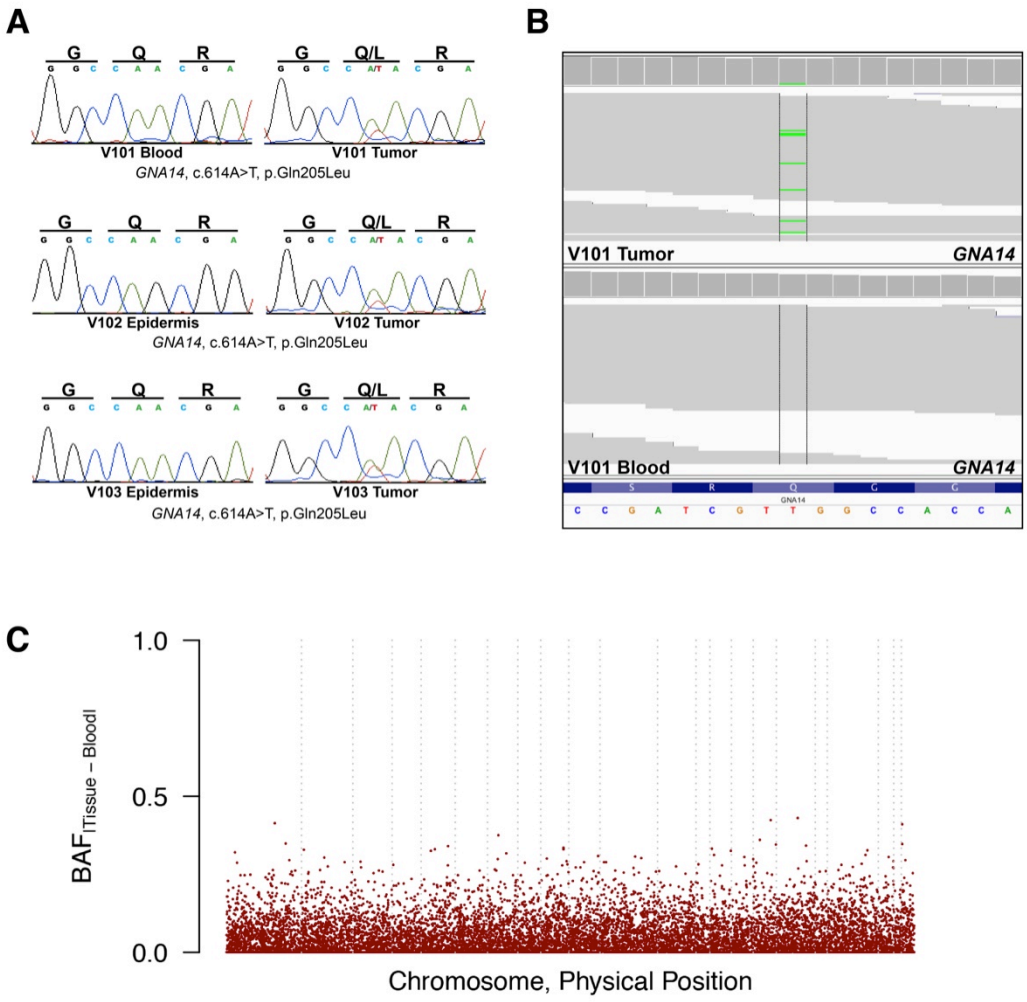

Figure S2. *GNA14* c.614A>T (p.Gln205Leu) mutation in vascular tumors. (A) Sanger sequencing traces show somatic *GNA14* c.614A>T (p.Gln205Leu) mutation in all 3 samples. **(B)** Integrated genome viewer (IGV) plots of exome sequencing data from V101 show 7/78 (9%) and 0/96 non-reference reads in tumor and blood, respectively. **(C)** Plot of B-allele frequency (BAF) demonstrates no segments of loss-of-heterozygosity or copy number variation in V101. Dotted lines separate individual chromosomes.

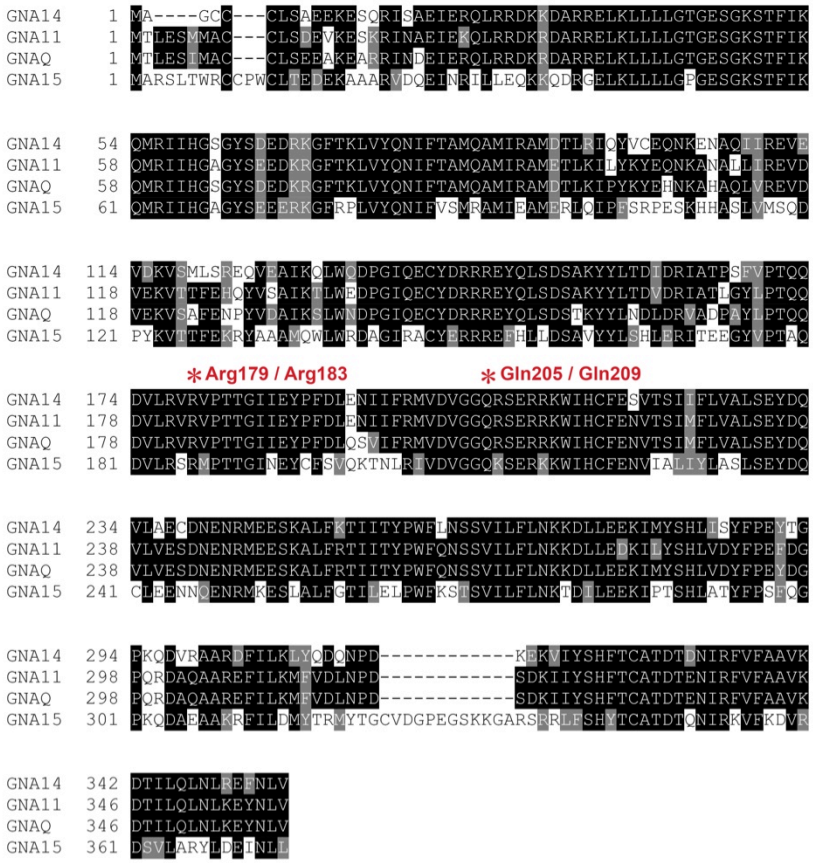

Figure S3. Sequence homology among members of the Gαq family. Arginine at positions 179 (GNA14) and 183 (GNA11) and glutamine at positions 205 (GNA14) and 209 (GNA11) (red asterisks) are conserved among all Gαq members.

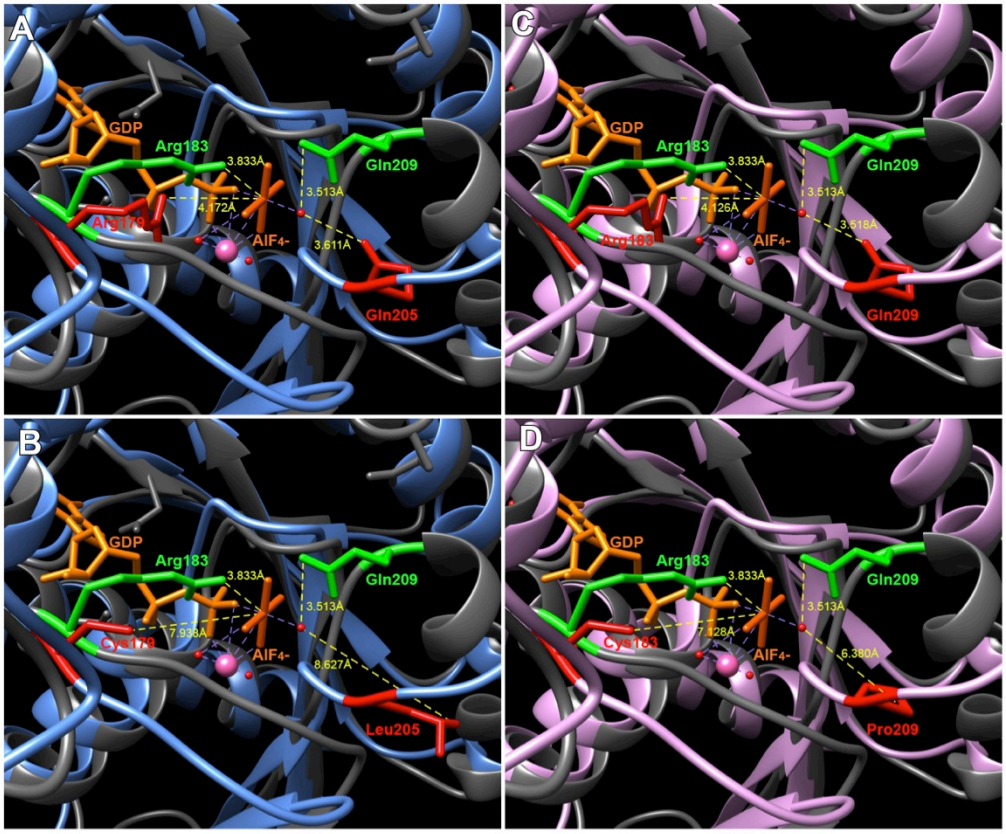

Figure S4. *GNA14* and *GNA11* mutations disrupt stabilization within the GTPase catalytic core. Phyre2 was employed to construct a theoretical model of GNA14 (A,B, blue) and GNA11 (C, D, pink) GTPase domains, which were overlaid with an established GNAQ template (A-D, grey). Residues in which mutation causes vascular tumors are highlighted in red (GNA14 and GNA11), and green (GNAQ). Molecular distance from stabilized moieties are labeled (yellow dashed lines). The transition state of bound GDP-AlF_4^- (orange)—representing GTP—undergoing hydrolysis is stabilized (purple dashed lines) by Mg^{2+} (pink sphere) and water moieties (red spheres) in the catalytic core. **(A)** Native GNA14 showing arginine 179 and glutamine 205, with corresponding GNAQ arginine 183 and glutamine 209. GNA14 arginine 179, like GNAQ arginine 183, stabilizes the leaving γ-phosphate, and in its native state, is 4.172Å from AlF_4^-. GNA14 glutamine 205, like GNAQ glutamine 209, stabilizes the water moiety driving hydrolysis of the γ-phosphate, and is 3.611Å away. **(B)** GNA14 with both p.Arg179Cys and p.Gln205Leu protein changes, with corresponding native GNAQ residues. Cysteine 179 and leucine 205 are distanced further from the γ-phosphate at 7.938Å and 8.627Å, respectively, and lose their stabilizing amide groups. **(C)** Native GNA11 with arginine 183 and glutamine 209, and corresponding residues in GNAQ. GNA11 arginine 183 is 4.126Å from AlF_4^-, while GNA11 glutamine 209 is 3.518Å from the nucleophilic water molecule. **(D)** GNA11 with p.Arg183Cys and p.Gln209Pro and corresponding native GNAQ residues shows GNA11 mutant residues are further away, with cysteine 183 at 7.128Å, and proline 209 at 6.380Å.

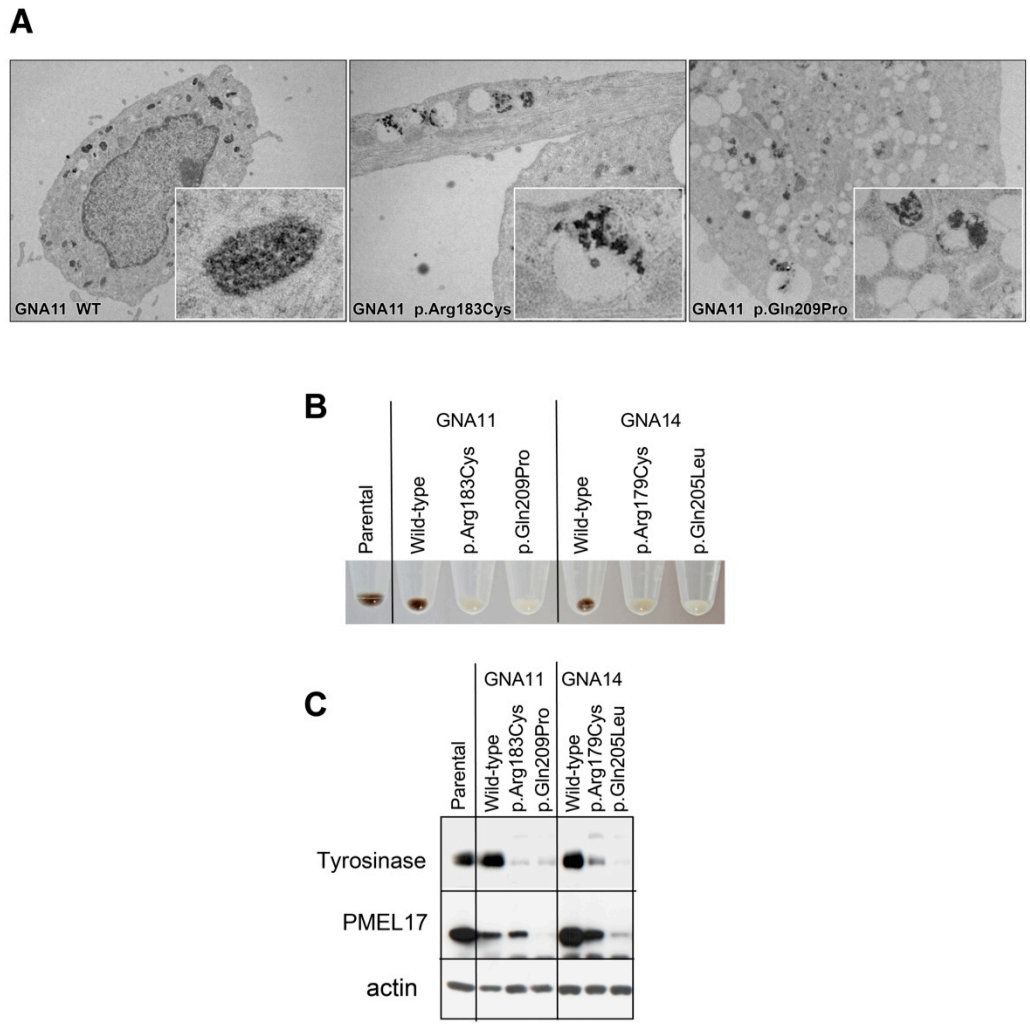

Figure S5. Activating *GNA11* and *GNA14* mutations result in loss of pigment in NBMELs. (A) Electron microscopy of NBMELs (GNA11 wild type, p.Arg183Cys, and p.Gln209Pro shown as representative) demonstrates melanosome degradation within vacuolar structures in the mutants, resulting in loss of cellular pigment (**B)**. **(C)** *GNA11* and *GNA14* mutations lead to lower levels of tyrosinase and Pmel17, markers of melanogenesis and intact melanosomes, respectively. The membrane was probed with antibodies against tyrosinase (T311, NeoMarker) and Pmel17,[1] and β-Actin (A1978, Sigma-Aldrich) as control for protein loading.

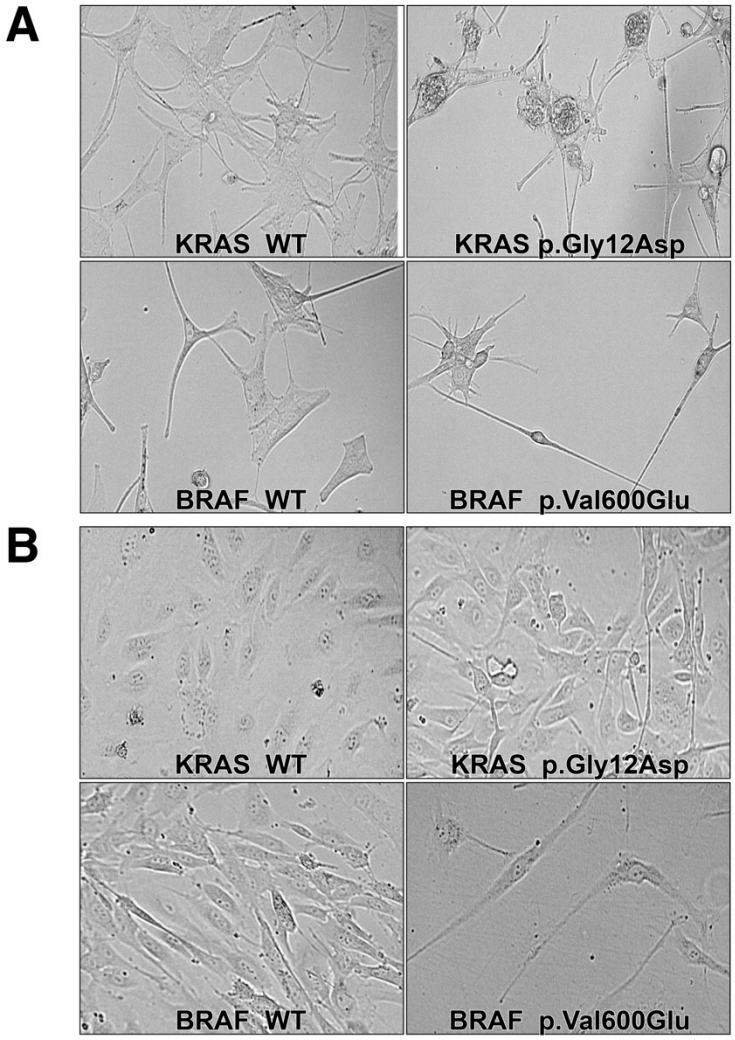

Figure S6. Activating *KRAS* and *BRAF* mutation in NBMEL and HUVEC lead to changes in morphology. (A) NBMELs expressing *KRAS* wild type and c.35G>A (p.Gly12Asp) and *BRAF* wild type and c.1799T>A (p.Val600Glu) mutation. (**B)** HUVECs expressing *KRAS* and *BRAF* wild type and mutation.

Sample	Mean Coverage	Bases Covered >8x	Bases Covered >20x	Mean Read Length
V101 Tissue	94x	97%	92%	74 bases
V101 Blood	89x	98%	91%	74 bases
V104 Tissue	68x	97%	88%	74 bases

Table S1. Exome coverage statistics. In all samples, >97% of coding regions are covered >8x, sufficient for analysis. 74bp paired-end sequencing of tissue and blood from V101 and tissue from V104 was performed by shearing and barcoding genomic DNA, followed by capture using Roche EZ Exome V3 capture probes. Sequencing was performed on the Illumina HiSeq 2500, with tissue samples run at 4 per lane, and blood run at 6 per lane. Sequence was aligned to the hg19 reference using BWA-MEM, trimmed, and PCR duplicates removed using Picard. BAM files were calibrated using GATK.

Filter	V101
All SSNVs	37
In exons/splice Site	20
Nonsynonymous	10
<0.1% Prevalence in ExAC	1 (*GNA14*)
Fisher's Test p-value < 1.0×10^{-2}	1 (*GNA14*)

Table S2. Somatic single nucleotide variant (SSNV) filtering. Somatic mutations were identified by employing a Perl script alongside MuTect. Called SSNVs were filtered to exclude intronic and intergenic variants, synonymous mutations, and mutations listed in ExAC, 1000 Genomes, the NHLBI Exome Variant Server, and dbSNP control datasets. The remaining variants were visualized using Integrative Genome Viewer (IGV) to inspect for mismapped reads. The single remaining *GNA14* mutation was validated with Sanger sequencing, and confirmed via laser capture microdissection in V102 and V103 (Figure S2).

SUPPLEMENTAL REFERENCES

1. Lee, Z.H., Hou, L., Moellmann, G., Kuklinska, E., Antol, K., Fraser, M., Halaban, R., and Kwon, B.S. (1996). Characterization and subcellular localization of human Pmel 17/silver, a 110-kDa (pre)melanosomal membrane protein associated with 5,6,-dihydroxyindole-2-carboxylic acid (DHICA) converting activity. The Journal of investigative dermatology 106, 605-610.